

# Internal Friction and Vulnerability of Mixed Alkali Glasses

Robby Peibst, Stephan Schott, and Philipp Maass

*Institut für Physik, Technische Universität Ilmenau, 98684 Ilmenau, Germany\**

(Dated: February 24, 2005)

Based on a hopping model we show how the mixed alkali effect in glasses can be understood if only a small fraction  $c_V$  of the available sites for the mobile ions is vacant. In particular, we reproduce the peculiar behavior of the internal friction and the steep fall (“vulnerability”) of the mobility of the majority ion upon small replacements by the minority ion. The single and mixed alkali internal friction peaks are caused by ion-vacancy and ion-ion exchange processes. If  $c_V$  is small, they can become comparable in height even at small mixing ratios. The large vulnerability is explained by a trapping of vacancies induced by the minority ions. Reasonable choices of model parameters yield typical behaviors found in experiments.

PACS numbers: 66.30.Dn, 66.30.Hs

The mixed alkali effect (MAE) is a key problem for understanding ion transport processes in glasses and refers to strong changes in transport properties upon mixing of two types of mobile ions (for reviews, see [1, 2]). Fundamental for the MAE is the behavior of the tracer diffusion coefficients  $D_A$  and  $D_B$  of two types of ions A and B. With increasing number fraction  $x$  of B ions, i.e. with successive replacement of A by B ions,  $D_A$  decreases while  $D_B$  increases. These changes are reflected in the activation energies  $E_{A,B}(x) \sim -k_B T \log D_{A,B}(x)$ , so that at low temperatures  $D_{A,B}(x)$  vary by many orders of magnitude. As a consequence, the ionic conductivity  $\sigma(x) \sim (1-x)D_A(x) + xD_B(x)$  runs through a deep minimum close to the intersection point of  $D_A$  and  $D_B$ .

Much progress was made in the past to explain the MAE [3, 4, 5, 6, 7, 8, 9, 10, 11, 12]. EXAFS [13] and NMR measurements [14], and in particular recent analyses of neutron and x-ray scattering data with the reverse Monte Carlo technique [10] support the picture that a structural mismatch effect leads to distinct preferential diffusion pathways for each type of mobile ion. The connectivity and interference of these pathways determines the long-range ion mobilities. On this theoretical basis alone, however, main properties of the MAE are still not well understood.

One property is the large “vulnerability”, that means the steep decrease of the diffusion coefficient of the majority ion, e.g. A, with beginning replacement by the minority ion B [15, 16]. In many mixed alkali glasses,  $\ln D_A(x)$  is a convex function for small  $x$ , reflecting that  $E_A(x)$  is a concave function in these systems [17, 18]. Why is the increase of  $E_A$  largest at beginning replacement, where the influence of the minority ion should be weak?

Another quantity poorly understood so far is the internal friction (for a review, see [19]). Measurements on mixed alkali glasses show that the ionic motion leads to two mechanical loss peaks, a single alkali peak (SP) and a mixed alkali peak (MP). The peak frequency  $\tau_s^{-1}$  of the SP has (nearly) the same activation energy  $E_s$  as the diffusivity of the more mobile ion, while the lower peak

frequency  $\tau_m^{-1}$  of the MP exhibits an activation energy  $E_m$  that is not simply related to that of the mobility of the less mobile ion. Particularly puzzling is that the height  $H_m$  of the MP can be comparable to the height  $H_s$  of the SP even at very small  $x$ , and that  $H_m$  becomes larger the more similar the two types of ions are [20].

In this Letter we show that these peculiar behaviors can be explained, if the fraction  $c_V$  of vacant sites for the mobile ions is small. Small values  $c_V = 5 - 10\%$  have been found recently in molecular dynamics simulations [21, 22], and should be expected also on general grounds, since empty sites correspond to local structural configuration of high energy [23]. Here we argue that the experimental results for the internal friction provide independent support for this feature.

To reason that conjecture, we note (see eq. (2) below) that the SP and MP can be attributed to processes, where the more mobile ions (e.g. A) exchange sites with vacancies (AV exchange), and where the A ions exchange sites with B ions (AB exchange). When denoting by  $c_{A,B}$  the fractions of sites occupied by A, B ions, a mean-field argument then predicts that  $H_s \propto c_A c_V$  and  $H_m \propto c_A c_B$  should become comparable if  $c_V \simeq c_B$ . Therefore, if it is possible to find  $H_m \simeq H_s$  at small  $x$ , where  $c_B \sim x$  is small,  $c_V$  must be small also. Indeed, we will show in the following that this rough argument can be substantiated.

First we are confronted with the general problem whether the mismatch concept is sustainable as mechanism for the MAE if  $c_V$  is small. To this end we investigate a lattice model, where the rate  $w_{ij}^\alpha$  for a jump of an  $\alpha$  ion ( $\alpha = A, B$ ) from site  $i$  to a nearest neighbor site  $j$  is determined by the site and barrier energies

$$\epsilon_i^\alpha = -\epsilon_{\text{mis}}^\alpha \mu_i^\alpha, \quad u_{ij}^\alpha = u_0^\alpha + \frac{u_{\text{mis}}^\alpha}{2} (\mu_i^\beta + \mu_j^\beta). \quad (1)$$

The mismatch effect is taken into account via the mismatch energies  $\epsilon_i^\alpha > 0$ ,  $u_{\text{mis}}^\alpha > 0$ , and the structural variables  $\mu_i^\alpha$ ,  $0 \leq \mu_i^\alpha \leq 1$  that specify the  $\alpha$ -character of site  $i$ . A site  $i$  with large  $\mu_i^\alpha$  has a local environment favorably accommodated to an  $\alpha$  ion and hence a low

energy  $\epsilon_i^\alpha$ . Large values of  $\mu_i^A$  imply a small value of  $\mu_i^B$  and vice versa. This is accounted for by taking opposing mean values  $\bar{\mu}_i^A = 1 - \bar{\mu}_i^B$  in the distributions of the  $\mu_i^\alpha$  (see below). Below a threshold value  $\mu_c^\alpha$ , sites lose their identity and we require the energy to saturate ( $\epsilon_i^\alpha = -\epsilon_{\text{mis}}\mu_c^\alpha$  for  $\mu_i^\alpha \leq \mu_c^\alpha$ ).

The barriers  $u_{ij}^\alpha$  in eq. (1) contain a bare structural barrier  $u_0^\alpha$  (characterizing the activation energy in the pure systems) and a mismatch barrier that becomes higher with increasing “foreign”  $\beta (\neq \alpha)$ -characters of the initial and target sites involved in a jump of an  $\alpha$  ion. This is necessary in order to obtain low mobilities for the minority ion in the dilute regime [24]. Within an Anderson-Stuart like picture [25] it can be physically understood by the fact that larger minority ions have to bring up an additional elastic strain energy when open up doorways, and that smaller minority ions have to surmount a higher saddle point energy associated with the Coulomb potential of the counter ions.

The disorder in the glass is reflected in the distributions of the  $\mu_i^\alpha$ . Due to the local accommodation of the network structure to the ions in course of the freezing process, the numbers of sites with large  $\mu_i^A$  and  $\mu_i^B$  scale with  $(1-x)$  and  $x$ , respectively. In addition we take into account short-range correlation between the  $\mu_i^\alpha$ . A convenient (technical) way to generate corresponding distributions (the detailed form is not important here) is as follows: We draw  $\mu_i^\alpha$  from truncated Gaussians ( $p(\mu_i^\alpha) \propto \exp[-(\mu_i^\alpha - \bar{\mu}_i^\alpha)^2/2\Delta_\alpha^2]$  for  $\mu_i^\alpha \in [0, 1]$ ) with  $\bar{\mu}_i^A = \sum_j \eta_j/(z+1) = 1 - \bar{\mu}_i^B$ , where the sum runs over site  $i$  and its nearest neighbors, and  $\eta_j$  are random binary numbers equal to one with probability  $(1-x)$ .

Kinetic Monte Carlo simulations are performed in a simple cubic lattice with periodic boundary conditions, using Metropolis hopping rates  $w_{ij}^\alpha = \nu_\alpha \exp(-u_{ij}^\alpha/k_B T) \min(1, \exp[-(\epsilon_j^\alpha - \epsilon_i^\alpha)/k_B T])$  ( $\nu_\alpha$  are attempt frequencies). We choose  $c_V = 0.05$  and consider, for computational convenience, a symmetric set of parameters  $\nu_A = \nu_B \equiv \nu$ ,  $\epsilon_{\text{mis}}^A = \epsilon_{\text{mis}}^B \equiv \epsilon_{\text{mis}}$ , ... To determine the tracer diffusion coefficients and internal friction as functions of  $x$  and reduced temperature  $\theta \equiv k_B T/\epsilon_{\text{mis}}$ , we fix the remaining parameters to  $\mu_c = 2/7$ ,  $\Delta = 1/14$ , and  $u_{\text{mis}} = 0.7\epsilon_{\text{mis}}$ . The parameter  $\epsilon_{\text{mis}}$  characterizes the difference between the two types of mobile ions (e.g. with respect to size).

Figure 1a shows the normalized diffusion coefficient  $D_A(x)/D_A(0)$  as a function of  $x$  for 5 different  $\theta$  [due to the symmetric parameters we do not plot  $D_B(x) = D_A(1-x)$ ]. The curves exhibit the typical behavior found in experiment:  $D_A(x)$  decreases by many orders of magnitude when A ions are replaced by B ions. This effect becomes stronger with lower temperature or stronger difference  $\epsilon_{\text{mis}}$  between the two types of mobile ions, i.e. with larger  $\theta = k_B T/\epsilon_{\text{mis}}$ . We thus conclude that the mismatch concept is sustainable for small  $c_V$ .

In particular,  $\log[D_A(x)/D_A(0)] = -E_A(x)/k_B T$ , ex-

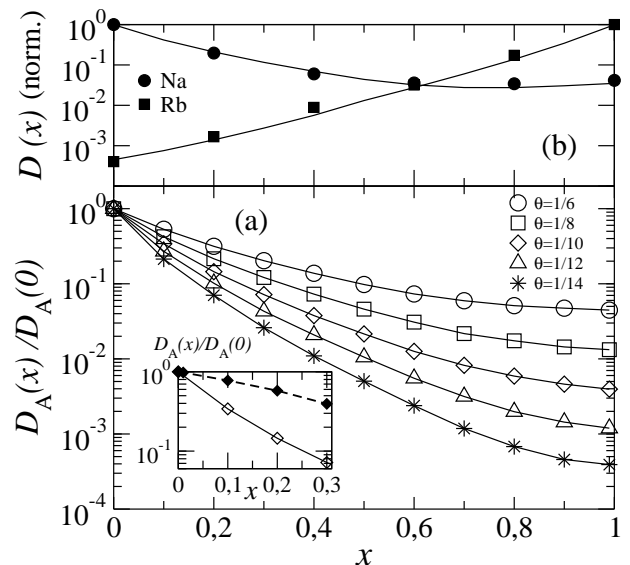


FIG. 1: (a) Normalized diffusion coefficient  $D_A(x)/D_A(0)$  of A ions for 5 different reduced temperatures  $\theta = k_B T/\epsilon_{\text{mis}}$ . The inset shows  $D_A(x)$  for small  $x$  at  $\theta = 1/10$  (open symbols) in comparison with the results in the absence of a correlation induced trapping effect (full symbols). (b) Measured data (symbols) for  $(1-x)\text{Na}_2\text{O}-x\text{Rb}_2-4\text{B}_2\text{O}_3$  glasses at 652K (redrawn from [18]) and fit by the model (lines) with  $\theta = 1/9$  and asymmetric mismatch barriers  $u_{\text{mis}}^B = 2u_{\text{mis}}^A = \epsilon_{\text{mis}}$ .

hibits a convex curvature for small  $x$ , and  $E_A(x)$  a concave curvature (see Fig. 4a; note that one must add  $u_0$  to obtain the total activation energy  $E_A^{\text{tot}}(x) = E_A(x) + u_0$ ). The large vulnerability is caused by a trapping effect: For small  $x$ , there exist regions in the glass where the network structure tended to accommodate to the “foreign” B ions. Because of the spatial correlations, the regions consist of several sites with smaller A character  $\mu_i^A$  than on average. These sites are not only favorably occupied by B ions, but also favorably occupied by vacancies, because this allows more of the majority A ions to occupy well accommodated sites with large  $\mu_i^A$  close to one. Vacancies hence become trapped in regions more favourably accommodated to the the foreign B ions and they have to bring up an additional activation energy to promote the diffusion of A ions. The corresponding reduction of  $D_A(x)$  is strongest for  $x \rightarrow 0$ , since with increasing  $x$  the number of sites with values  $\mu_i^A$  close to one decreases. The importance of the trapping effect [26] is demonstrated in the inset of Fig. 1a, where  $D_A(x)$  is shown in comparison with the curve obtained in the absence of spatial correlations ( $\bar{\mu}_i^A = \eta_i^A$  instead of  $\bar{\mu}_i^A = \sum_j \eta_j/(z+1)$ ) but otherwise the same parameters).

Fig. 1a resembles well the experimental behavior. By choosing asymmetric parameters one can reproduce measured curves as shown in Fig. 1b with reasonable parameter values (if we require  $\theta = 1/9$  in Fig. 1b to represent the experimental temperature 652K, we would obtain a mismatch energy  $\epsilon_{\text{mis}} = 0.5\text{eV}$ ). A detailed fitting to ex-

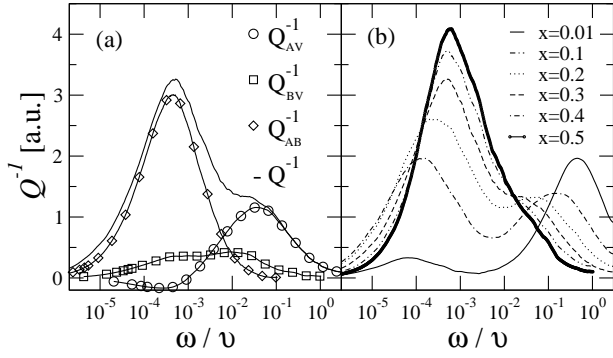


FIG. 2: (a) Internal Friction  $Q^{-1}$  and spectral components (cf. eq. 2) as a function of  $\omega$  for  $x = 0.3$  and  $\theta = 1/10$ . (b) Change of the internal friction  $Q^{-1}$  with  $x$  for  $\theta = 1/10$ .

perimental results, however, is not our aim here (and has limitations due the simplicity of the model).

Rather, we next explore how the behavior in the internal friction  $Q^{-1}(\omega, T)$  can be understood. To this end, we consider a small modulation  $\Delta\epsilon_i^\alpha(t) = a_0 \Re[\chi_i^\alpha e^{-i\omega t}]$  of the site energies in response to an oscillatory shear stress with amplitude  $a_0$  and frequency  $\omega$  [27]. The complex coupling constants  $\chi_i^\alpha$  fluctuate due to the disorder in the glass. Without making specific assumptions regarding their correlation properties, we employ a random phase ansatz and regard them to be uncorrelated for different sites  $i$  and different types  $\alpha$ ,  $[\chi_i^\alpha \chi_j^{\beta*}]_{\text{av}} \propto \delta_{\alpha\beta} \delta_{ij}$ , and uncorrelated with the site energies of the unperturbed system  $[\chi_i^\alpha \epsilon_i^\alpha]_{\text{av}} = 0$  ( $[\dots]_{\text{av}}$  denotes a disorder average). Introducing the occupation numbers  $n_i^\alpha(t)$ , i.e.  $n_i^\alpha(t) = 1$  if site  $i$  is occupied by species  $\alpha$  ( $\alpha = A, B, V$  here) at time  $t$  and zero else, linear response theory then expresses the internal friction in terms of the Fourier cosine transforms of the exchange correlation functions  $\langle n_i^\alpha(t) n_j^\beta(0) \rangle$  ( $\langle \dots \rangle$  denotes a thermal average). The result is

$$Q^{-1}(\omega, T) = \frac{\kappa \omega}{k_B T} \left[ \sum_{\alpha=A,B} c_{\alpha V} S_{\alpha V} + 2c_{AB} S_{AB} \right] \quad (2)$$

$$S_{\alpha\beta}(\omega, T) = \int_0^\infty dt C_{\alpha\beta}(t) \cos(\omega t), \quad (3)$$

where  $\kappa$  is constant [28],  $c_{\alpha\beta} = [\langle n_i^\alpha \rangle \langle n_i^\beta \rangle]_{\text{av}}$ , and  $C_{\alpha\beta}(t) = 1 - [\langle n_i^\alpha(t) n_i^\beta \rangle]_{\text{av}} / c_{\alpha\beta}$  are the normalized exchange correlation functions [ $C_{\alpha\beta}(0) = 1$  and  $C_{\alpha\beta}(t \rightarrow \infty) = 0$ ].

Figure 2a shows  $Q^{-1}$  as a function of  $\omega$  for  $x = 0.3$  and  $\theta = 1/10$ , together with the spectral components  $Q_{\alpha\beta}^{-1} \propto (\omega/\theta) c_{\alpha\beta} S_{\alpha\beta}$  in eq. (2). Two arise from exchange processes of the ions with the vacancies (AV and BV exchange) and one arises from exchange processes of the two types of ions (AB exchange). The exchange of vacancies with the majority ions (AV) leads to the SP and the AB exchange to the MP, while the BV exchange yields a broad spectral contribution that is masked by the SP and MP, and cannot be resolved in  $Q^{-1}$ . The overall behavior of  $Q^{-1}$  with varying  $x$  for  $\theta = 1/10$  is shown in

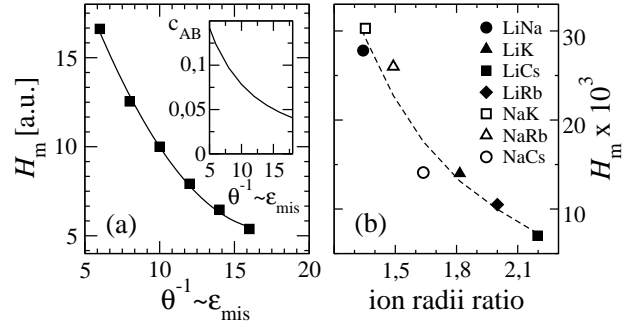


FIG. 3: (a)  $H_m$  in dependence of  $\theta^{-1} = \epsilon_{\text{mis}}/k_B T$  at  $x = 0.5$ . The inset shows the decrease of  $c_{AB}$  with increasing  $\theta^{-1} \propto \epsilon_{\text{mis}}$  (from analytical calculation). (b)  $H_m$  as a function of ion radii ratio of various mixed alkali pairs for  $x = 0.5$  and  $\omega/2\pi = 0.4\text{Hz}$  fixed.

Fig. 2b. Due to the small  $c_V$ , the MP can be well identified already for  $x = 0.01$ , in agreement with the argument given above. With increasing  $x$  the MP becomes higher and moves towards larger frequencies, while the SP becomes lower and moves towards smaller frequencies. At  $x = 0.5$  the SP cannot be resolved any longer.

Remarkably, also the puzzling rise of the height  $H_m$  with increasing similarity of the two types of mobile ions (i.e. decreasing  $\epsilon_{\text{mis}}$ ) is reproduced, see Fig. 3a.  $H_m$  at  $x = 0.5$  becomes higher with decreasing  $\epsilon_{\text{mis}}$  (we regard  $T$  to be fixed here). The reason for this behavior lies in the weighting of the AB peak by the disorder averaged product  $c_{AB} = [\langle n_i^A \rangle \langle n_i^B \rangle]_{\text{av}}$  of the equilibrium occupations  $\langle n_i^A \rangle$ ,  $\langle n_i^B \rangle$  in eq. (2). With increasing mismatch  $\epsilon_{\text{mis}}$ , A and B ions share the same sites with lower probability (see inset of Fig. 3a) and accordingly  $H_m$  decreases. The behavior is reminiscent to the variation of  $H_m$  with the fraction of ion radii observed in experiments at  $x = 0.5$  for a fixed frequency, see Fig. 3b [29].

When denoting by  $E_{\alpha\beta}$  the activation energies of the  $Q_{\alpha\beta}^{-1}$  peak frequencies  $\tau_{\alpha\beta}^{-1}$ , we can define by  $E_s = \min(E_{AV}, E_{BV})$  and  $E_m = E_{AB}$  the activation energies of the SP and MP. The activation energies  $E_{\alpha\beta}$  obtained from Arrhenius plots (for the same  $\theta$  values as in Fig. 1) are shown in Fig. 4a together with the diffusion activation energies  $E_{<} \equiv \min(E_A, E_B)$  and  $E_{>} \equiv \max(E_A, E_B)$  of the more and less mobile ion. We find that  $E_s (= \min(E_{AV}, E_{BV}))$  follows closely  $E_{<}$ , in agreement with measurements [19]. By contrast,  $E_m (= E_{AB})$  differs from  $E_{>}$ . The deviations found in Fig. 4a are similar to those found in experiments, see Fig. 4b [30].

To show  $Q^{-1}$  as function of temperature for fixed frequency, as typically obtained in experiments, we use time-temperature scaling to transform  $Q^{-1}$  from frequency to temperature space. Taking the  $\theta$  values from Fig. 1a, we first checked, that a scaling  $\omega S_{\alpha\beta}(\omega, T) = F_{\alpha\beta}(\omega \tau_{\alpha\beta}(T))$  is approximately valid. By applying this scaling we then replot  $Q^{-1}$  from Fig. 2b as function of  $T$  in Fig. 4c for small  $x$  and parameter values  $\epsilon_{\text{mis}} = 1\text{eV}$ ,

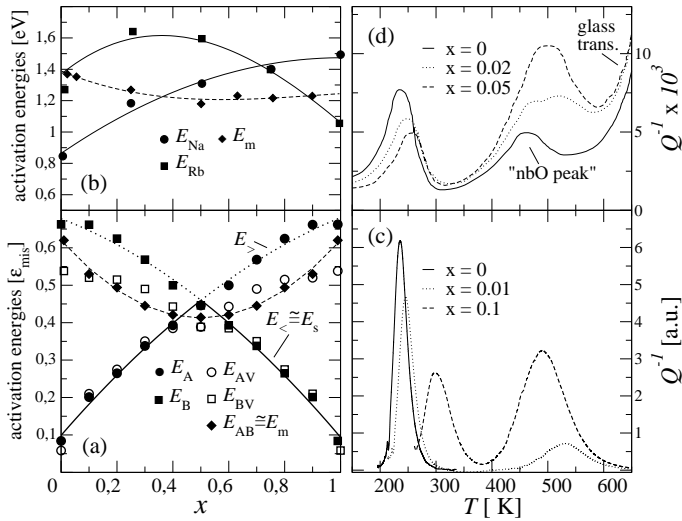


FIG. 4: (a) Activation energies of the tracer diffusion coefficients shown in Fig. 1, and of the spectral components of the internal friction. (b)  $E_{Na}$ ,  $E_{Rb}$ , and  $E_m$  in  $(1-x)\text{Na}_2\text{O}-x\text{Rb}_2\text{O}-3\text{SiO}_2$  glasses (redrawn from [17]). (c)  $Q^{-1}$  calculated from Fig. 2 after applying time-temperature scaling for  $\epsilon_{\text{mis}} = 2u_0 = 1\text{eV}$  and  $\omega/\nu = 10^{12}$  (see text). (d)  $Q^{-1}$  in  $(1-x)\text{Na}_2\text{O}-x\text{Rb}_2\text{O}-3\text{SiO}_2$  glasses for  $\omega/2\pi = 0.4\text{Hz}$  (redrawn from [17]).

$u_0 = 0.5\text{eV}$ , and  $\omega/\nu = 10^{-12}$ . These values yield activation energies  $E_A^{\text{tot}}(x) = E_A + u_0 \simeq 0.6 \dots 1.2\text{eV}$  comparable to those found in experiments, cf. Fig. 4b. The choice  $\omega/\nu = 10^{-12}$  corresponds to  $\omega \simeq 1\text{Hz}$ , when  $\nu \simeq 10^{12}\text{Hz}$  is a typical attempt frequency. Using this rough parameter estimate, peak temperatures in Fig. 4c are obtained that reflect the experimental scenario in Fig. 4d [note that the glass transition and the “non-bridging oxygen” (nbO) peak [19] are not taken into account in the present approach].

In summary, we have shown how the mixed alkali effect in glasses, including the vulnerability and the peculiar features of the internal friction, can be understood based on the mismatch effect in the presence of a small vacancy concentration. Due to the small  $c_V$ ,  $H_m$  can become comparable to  $H_s$  even at small concentrations of the minority ion, and  $H_m$  increases, when it becomes easier for both types of ions to share the same sites. The large vulnerability can be connected to a trapping of vacancies induced by the minority ions. Reasonable choices of parameters allowed us to faithfully reproduce typical behaviors found in experiments.

We thank W. Dieterich, J. Habasaki, and M. D. Ingram for valuable discussions.

\* Electronic address: Philipp.Maass@tu-ilmenau.de;  
URL: <http://www.tu-ilmenau.de/theophys2>

[1] D. E. Day, J. Non-Cryst. Solids **21**, 343 (1976).

- [2] M. D. Ingram, Glstech. Ber. Glass Sci. Technol. **67**, 151 (1994).
- [3] P. Maass, A. Bunde, and M. D. Ingram Phys. Rev. Lett. **68**, 3064 (1992); A. Bunde, M. D. Ingram, and P. Maass J. Non-Cryst. Solids **172-174**, 1222 (1994).
- [4] A. Hunt, J. Non-Cryst. Solids **175**, 129 (1994).
- [5] G. N. Greaves and K. L. Ngai, Phys. Rev. B **52**, 6358 (1995).
- [6] M. Tomozawa, Solid State Ionics **105**, 249 (1998).
- [7] B. M. Schulz, M. Dubiel, and M. Schulz, J. Non-Cryst. Solids **241**, 149 (1999).
- [8] P. Maass, J. Non-Cryst. Solids **255**, 35 (1999).
- [9] R. Kirchheim, J. Non-Cryst. Solids **272**, 85 (2000).
- [10] J. Swenson, A. Matic, C. Karlsson, L. Börjesson, C. Meneghini, and W. S. Howells, Phys. Rev. B **63**, 132202 (2001).
- [11] J. Swenson and S. Adams, Phys. Rev. Lett. **90**, 155507 (2003).
- [12] A. Bunde, M. D. Ingram, and S. Russ, Phys. Chem. Chem. Phys. **6**, 3663 (2004).
- [13] G. N. Greaves *et al.*, Phil. Mag. A **64**, 1059 (1991).
- [14] B. Gee, M. Janssen, and H. Eckert, J. Non-Cryst. Solids **215**, 41 (1997).
- [15] M. D. Ingram and B. Røling, J. Phys.: Condens. Matter **14**, 1 (2002).
- [16] C. T. Moynihan and A. V. Lesikar, J. Am. Ceram. Soc. **63**, 458 (1981).
- [17] G. L. McVay and D. E. Day, J. Am. Ceram. Soc. **53**, 508 (1970).
- [18] S. Voss, Á. W. Imre, and H. Mehrer, Phys. Chem. Chem. Phys. **6**, 3669 (2004); S. Voss, F. Berkemeier, Á. W. Imre, and H. Mehrer, Z. Phys. Chem. **218**, 1353 (2004).
- [19] W. A. Zdaniewski, G. E. Rindone, and D. E. Day, J. Mater. Sci. **14**, 763 (1979).
- [20] D. E. Day, in *Amorphous Materials*, eds. R. W. Douglas and B. Ellis (Wiley Interscience, New York, 1972), p. 39.
- [21] H. Lammert, M. Kunow, and A. Heuer, Phys. Rev. Lett. **90**, 215901 (2003).
- [22] J. Habasaki and Y. Hiwatari, Phys. Rev. B **69**, 144207 (2004).
- [23] J. C. Dyre, J. Non-Cryst. Solids **324**, 192 (2003).
- [24] When a mismatch in the energy barriers is absent, the minority ions would, in the dilute limit, be driven away from their favorable low-energy sites by entropic forces and assume mobilities comparable to the majority ions.
- [25] O. L. Anderson and D. A. Stuart, J. Am. Ceram. Soc. **37**, 573 (1954).
- [26] In the present model the trapping effect is caused by correlations in the structural properties. Alternatively, a trapping of vacancies can be caused by ion-ion interactions, as, for example, in the MAE seen in crystalline ionic conductors with  $\beta''\text{-Al}_2\text{O}_3$  structure [see M. Meyer *et al.*, Phys. Rev. Lett. **76**, 2338 (1996)].
- [27] D. Knödler, O. Stiller, and W. Dieterich, Phil. Mag. B **71**, 661 (1995).
- [28] For the coefficient  $\kappa$  one finds  $\kappa = 2\pi[|\chi_i^\alpha|^2]_{\text{av}}/M'a^3$ , where  $M'$  is the real part of the shear modulus, which is governed by the (elastic) network response and thus very weakly dependent on frequency ( $a$ : mean jump distance).
- [29] When the ion ratio approaches one (as for the K/Rb pair), the correlation to  $\epsilon_{\text{mis}}$  should become weaker and other properties (e.g. polarizabilities) will dominate  $\epsilon_{\text{mis}}$ .
- [30] It is interesting to note that the activation energy corresponding to the exchange of vacancies with the less mo-

mobile ions does not follow the diffusion activation energy of the less mobile ion.